

Theory of surface plasmon-polariton amplification in planar structures incorporating dipolar gain media

Israel De Leon* and Pierre Berini†

School of Information Technology and Engineering (SITE), University of Ottawa, 161 Louis Pasteur, Ottawa, Ontario, Canada K1N 6N5

(Received 13 June 2008; published 3 October 2008)

We investigate theoretically surface plasmon-polariton (SPP) amplification in planar metallic structures taking into account the nonuniformity of the gain medium close to the metal surface due to position-dependent dipole lifetime and pump irradiance. We propose a model that accounts for these nonuniformities and apply it to a physically realizable structure consisting of a thin silver film cladded on one side by a lossless dielectric and on the other by an optically pumped Rhodamine 6G dye solution. We study amplification of the supported long-range SPP mode and show that net amplification is possible at visible wavelengths using reasonable pump power and molecular concentration. It is shown that the gain nonuniformity close to the metal surface must be considered to describe adequately the SPP amplification phenomenon.

DOI: 10.1103/PhysRevB.78.161401

PACS number(s): 73.20.Mf, 78.20.Bh, 78.45.+h

Surface plasmon polaritons (SPPs) are electromagnetic waves coupled to free electron oscillations that propagate along the interface between a dielectric and a metal with a negative real part of permittivity.¹ Their unique properties offer promise for numerous applications.² Yet, a fundamental limitation is their short propagation length resulting from power dissipation in the metal. Recently, considerable efforts have been devoted to compensate for the SPP losses in planar structures by using gain media to achieve mode amplification.^{3–10} It has been suggested that incorporating gain in such structures could also lead to the realization of SPP lasers at visible wavelengths.^{11,12} Indeed, SPP lasers have already been demonstrated at midinfrared wavelengths.¹³ Improved resolution of near-field lenses through amplification of SPPs¹⁴ and the interaction of gain media with surface plasmons in metallic nanoparticles^{15,16} have been also investigated.

In this growing research area, understanding the characteristics of the gain medium close to the metal surface is of major importance. For this, two factors must be carefully considered. The first factor is the excited state lifetime of dipolar gain media such as organic dye molecules and rare-earth ions, or equivalently, the recombination lifetime of semiconductor gain media such as quantum wells and quantum dots. It is well known that these lifetimes are quenched by a metallic surface due to additional decay channels through which the dipole (or electron-hole pair) relaxes.^{17–19} This phenomenon certainly affects the gain available close to the metal. The second factor is the method used to pump the gain medium. In particular, for optically pumped gain media, the irradiance²⁰ distribution of the pump signal is generally not uniform near the metal. As a result of these factors, a uniform-gain picture is not adequate in the vicinity of a metallic surface.

In treating the amplification of SPP modes, the nonuniformity of the gain close to the metal has generally been neglected (in some cases justified) by assigning a uniform complex permittivity to the gain medium and solving Maxwell's equations in the active structure. A simplified approach was used by Okamoto *et al.*,¹¹ where the SPP gain is estimated by assuming a uniform gain medium and using bulk-plane-wave

amplification arguments. Winter *et al.*¹² further analyzed the structure proposed by Okamoto *et al.*,¹¹ pointing out the need to account for additional decay channels.

In this Rapid Communication, we investigate how SPP amplification in planar structures is affected by a nonuniform gain distribution close to the metal surface. We propose a theoretical model to describe this phenomenon in structures incorporating dipolar gain media. Our approach consists in obtaining the gain distribution near the metal surface employing position-dependent expressions for the dipole lifetime and pump irradiance. The former accounts for all of the decay channels through which the dipole relaxes and the latter accounts for the pump-signal interaction with the structure. The SPP mode amplification is then computed by solving Maxwell's equations in the active structure using the inhomogeneous complex permittivity describing the gain distribution. This concept can be extended to semiconductor gain media as well by representing adequately the gain distribution in the vicinity of the metal surface.

For the analysis we consider the structure shown in Fig. 1. It consists of a 20-nm-thick silver film extending infinitely over the (x, z) plane. The bottom cladding consists of 25 μm of CYTOP, a lossless dielectric, which in turn sits on a semi-infinite silicon substrate; the top surface is covered by Rhodamine 6G (R6G) dye molecules in a mixture of ethanol and methanol. A semi-infinite CYTOP superstrate lies on top of the dye solution, holding it to within a 5- μm -thick layer. Dye molecules are assumed to be excited from the top by a monochromatic pump signal of wavelength $\lambda_p=532$ nm [frequency-doubled Nd:YAG (yttrium aluminum garnet)],

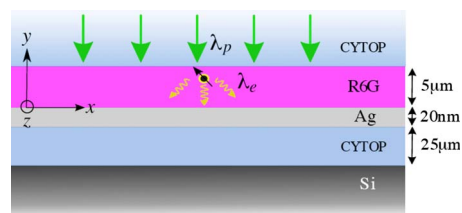


FIG. 1. (Color online) The SPP waveguide structure considered in this work.

TABLE I. Relative permittivities (ϵ_r) at $\lambda_p=532$ nm and $\lambda_e=560$ nm. *57% methanol 43% ethanol is assumed.

Material	$\epsilon_r(\lambda_p)$	$\epsilon_r(\lambda_e)$
Silver ²⁵	$-10.18-i0.8311$	$-11.68-i0.8283$
Silicon ²⁵	$17.22-i0.3646$	$16.42-i0.2936$
CYTOP ²⁶	1.8053	1.8039
Dye solvent* ²³	1.8068	1.8039

which is near the peak absorption of R6G. SPP mode amplification is analyzed at the peak emission wavelength of the dye, $\lambda_e=560$ nm. We approximate the parameters of R6G as those in pure methanol²¹ since the dye performs similarly in both solvents.²² We study the case where the real permittivity of the dye solution is matched to that of CYTOP at λ_e . This can be achieved using a solvent mixture of approximately 57% methanol and 43% ethanol.²³ Such a symmetric structure supports nonleaky short-range SPP (SRSP) and long-range SPP (LRSP) modes.²⁴ Table I lists the material relative permittivities at the two wavelengths of interest. The proposed structure and pumping arrangement are physically realizable and could serve directly as a validation vehicle for the theory proposed herein with the LRSP coupled in and out of the structure via end-fire coupling.

The basic electronic dynamics of organic dye molecules can be approximated by the rate equations of a four-level system.²⁷ The steady-state solution gives the following small signal amplification coefficient at λ_e :

$$\alpha_e = N \frac{I_p \tau \sigma_p \sigma_e - \sigma_a \hbar \omega_p}{\hbar \omega_p + I_p \tau \sigma_p}, \quad (1)$$

where N is the total molecular density, I_p is the pump irradiance, τ is the excited-state lifetime, σ_e and σ_a are, respectively, the emission and absorption cross sections at λ_e , σ_p is the absorption cross section at λ_p , ω_p is the pump angular frequency, and \hbar is the reduced Plank constant. This expression is valid for continuous-wave and pulsed pump signals provided that the pulse width is considerably longer than τ . To understand the gain distribution close to the metal we shall identify adequate expressions for τ and I_p .

Following the treatment by Ford and Weber¹⁷ we model the molecule as classical dipole and examine its excited state lifetime in the presence of a thin metal film. Far from the metal, the lifetime is unaffected and is given by the usual definition, $\tau_0 = [\gamma_{nr} + \gamma_r]^{-1} = \phi / \gamma_r$, where γ_r denotes the radiative decay rate, γ_{nr} accounts for all the nonradiative (NR) decay channels intrinsic to the dipole, and ϕ is the dipole's quantum efficiency ($\phi=0.9$ for the present case²¹). However, close to the metal film, γ_r is replaced by the sum of four decay channels that arise from coupling of the dipole to (1) LRSP and (2) SRSP modes, where the dipole emits a SPP instead a photon; (3) coupling to electron-hole (EH) pairs in the metal film, where the energy is directly transferred from the dipole to the metal in a dipole-dipole interaction; and (4) coupling to the radiation modes of the structure. The decay rates into these four channels are affected by the dipole's position and dipole-moment orientation, while γ_{nr} is as-

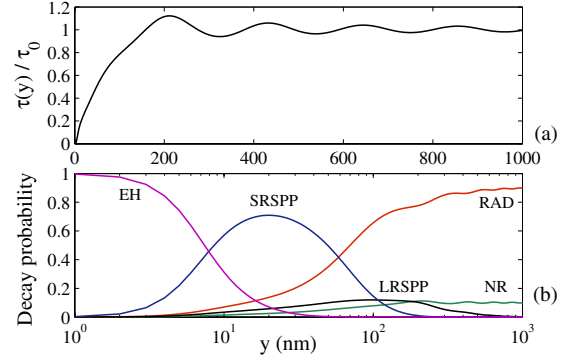


FIG. 2. (Color online) (a) Normalized lifetime computed using Eq. (3). (b) Decay probabilities into each decay channel.

sumed to be independent of the environment. For the structure under analysis, we write the position-dependent decay rate normalized to the decay rate far from the silver film as

$$\hat{\gamma}^{h,v}(y) = \hat{\gamma}_{nr} + \phi \sum_i^4 \hat{\gamma}_i^{h,v}(y), \quad (2)$$

where y is the dipole's position; $\phi \hat{\gamma}_i^{h,v}$ denotes the normalized decay rates of the four decay channels for (h) horizontal and (v) vertical dipole-moment orientations with respect to the metal plane; and $\hat{\gamma}_{nr} = 1 - \phi$ is the normalized nonradiative decay rate.

The rates in Eq. (2) are obtained by numerical integration of Eq. (3.30) in Ref. 17 using the local model for silver permittivity and the material permittivities of the structure at λ_e . The integral runs over all wave-vector components parallel to the silver plane, k_{\parallel} . We set its upper limit to $k_{\parallel} = 2.2k_F$ (k_F being the Fermi wave vector) to account approximately for electron screening, which becomes important when the dipole separation from the silver surface is less than a few nanometers. The limit employed corresponds to the upper limit of the EH excitation continuum in silver at λ_e .¹⁷

Averaging Eq. (2) over the dipole orientations yields the expression for the lifetime of an isotropically oriented dipole,

$$\tau(y) = \tau_0 \left[\frac{2}{3} \hat{\gamma}^h(y) + \frac{1}{3} \hat{\gamma}^v(y) \right]^{-1}. \quad (3)$$

Figure 2(a) shows the result of Eq. (3) normalized to τ_0 . Note that the lifetime is strongly quenched for distances below ~ 150 nm and it is practically unaffected when the distance reaches $1 \mu\text{m}$. The quenching and oscillatory features are due to the different competing decay channels previously mentioned. To understand the effect of each decay channel on the lifetime we show in Fig. 2(b) their decay probabilities. This probability is defined as the ratio of the particular decay rate over the total decay rate, both for an isotropic dipole. Note that coupling to EH pairs and to the SRSP mode dominate for distances below 60 nm, causing the strong lifetime quenching within this region. On the other hand, for distances between 60 and 150 nm, the lifetime quenching is mainly due to coupling to SRSP and LRSP modes. Finally, coupling to radiation modes (RAD) of the structure

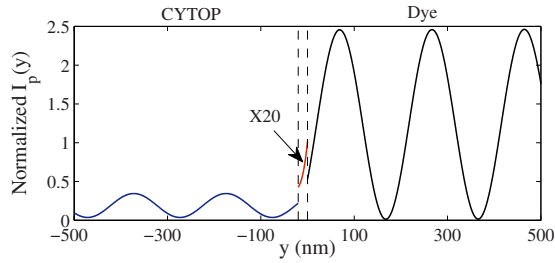


FIG. 3. (Color online) Normalized pump irradiance distribution in the vicinity of the silver film. The irradiance in the silver film is magnified 20 times.

and the NR relaxation dominate above 200 nm being only weakly affected by the LRSPP decay channel.

Although Eq. (3) denotes the lifetime of a *single* dipole, the same expression must hold for a homogeneously distributed collection of them assuming that the interactions between dipoles can be neglected. Such interactions have been observed under large dye concentrations. For R6G in methanol this effect is not significant for concentrations lower than ~ 5 mM.²¹

We now consider in some detail the spatial dependence of the pump signal. It is taken as a linearly polarized plane wave that illuminates the structure from the top with propagation direction normal to the metal surface. The electric-field distribution across the structure is computed rigorously with a matrix formalism.²⁸ In the calculations we use the material relative permittivities at λ_p and take the dye relative permittivity as $\epsilon_{r,p} = \epsilon'_{r,p} - iN\sigma_p(\epsilon'_{r,p})^{1/2}\lambda_p/2\pi$, where $\epsilon'_{r,p}$ is the relative permittivity of the dye solvent. Here, we assumed that all the dipoles are in the ground state. This approximation is well justified for a thin dye layer.

The pump irradiance distribution in each medium is computed as²⁹

$$I_p(y) = \frac{\text{Re}(\eta)}{2|\eta|^2} |E_p(y)|^2, \quad (4)$$

where $E_p(y)$ is the pump electric-field distribution and η is the medium's characteristic impedance. Figure 3 shows $I_p(y)$ in the vicinity of the silver film normalized to the irradiance of the incoming pump signal. The vertical dashed lines outline the silver film. The lower-cladding thickness was chosen to minimize the resonant coupling to the slab mode. In the dye, the irradiance follows a standing-wave pattern due to field reflection throughout the structure. It presents ~ 2.5 fold maxima, which enhances the population inversion in those regions. On the other hand, the minima are close to zero, suggesting that population inversion is not possible in those regions.

Substituting Eqs. (4) and (3) into Eq. (1) one obtains a local expression for the gain of the dye, $\alpha_e(y)$. Notice that dipoles in regions where $I_p(y) \approx 0$ or $\tau(y) \approx 0$ act merely as absorbers at λ_e since $\alpha_e(y) \approx -N\sigma_a$. The relative permittivity of the dye at λ_e is then

$$\epsilon_{r,e}(y) = \epsilon'_{r,e} + i\frac{\lambda_e}{2\pi} \alpha_e(y) \sqrt{\epsilon'_{r,e}}, \quad (5)$$

where $\epsilon'_{r,e}$ is the relative permittivity of the dye solvent.

TABLE II. MPG of the LRSPP for the cases under analysis.

Case	A	B	C	Passive
MPG[cm^{-1}]	2.9047	26.4756	22.3423	-105.3036

We proceed to study the amplification of SPP modes. The mode propagation is taken along the $+z$ axis having a complex phase of the form $\exp(-ikz)$, with $k = \beta + i\alpha$ being the complex propagation constant. Thus, a positive (negative) value for α indicates amplification (attenuation) as the mode propagates in the $+z$ direction. The inhomogeneous gain medium is treated as a multilayer structure by discretizing Eq. (5) along the y axis. Then, the transfer matrix method (TMM) (Ref. 30) is used to compute the SPP mode. We assume a R6G concentration of $N = 3$ mM ($\sim 1.8 \times 10^{18} \text{ cm}^{-3}$) and a pump irradiance of 210 kW/cm^2 . The parameters for R6G are taken from Ref. 21 as $\sigma_e = 3 \times 10^{-16} \text{ cm}^2$, $\sigma_p = 4 \times 10^{-16} \text{ cm}^2$, $\sigma_a = 1 \times 10^{-17} \text{ cm}^2$, and $\tau_0 = 3.9$ ns. The gain medium is segmented in 15 000 layers of equal thickness and the TMM analysis is carried out at λ_e using the corresponding material relative permittivities.

To visualize the impact of nonuniform gain distribution near the metal we consider three cases. Case (A) computes the SPP mode in the active structure taking into account both pump and lifetime position dependence. The other two cases use only a partial approach. Case (B) accounts for the pump distribution but assumes a uniform lifetime $\tau = \tau_0$, while case (C) assumes a uniform gain distribution, neglecting both pump and lifetime position dependence.

We shall focus on the nonleaky LRSPP mode supported by the structure. It has lower propagation loss than the SR-SPP mode, which makes it attractive for amplification and lasing applications. The results are summarized in Table II that lists the mode power gain, $\text{MPG} = 2 \text{ Im}(k)$, for each case. It also includes the value for the passive case, i.e., when no R6G molecules are present in the solvent. The mode effective index, $n_{\text{eff}} = \lambda_e \text{ Re}(k)/2\pi$, was evaluated as $n_{\text{eff}} = 1.3613$ for all the cases listed in Table II. We note that cases (B) and (C) give similar results, predicting MPG values around 25 cm^{-1} . However, the MPG value for (A) is approximately an order of magnitude smaller. In terms of pump requirements, we found that case (A) requires an extra $\sim 100 \text{ kW/cm}^2$ of irradiance to match the gain predicted by the other two cases.

To understand the difference in these results we consider Fig. 4. It shows the LRSPP mode and gain distributions for the three cases (the mode distribution is practically identical for the three cases). Since mode amplification is a stimulated emission process, it is necessary for the gain and mode distributions to overlap efficiently. For cases (B) and (C) the overlap turns out to be very similar, resulting in similar MPG values. On the other hand, for case (A), the gain is strongly suppressed due to the lifetime quenching. In fact, the medium becomes absorptive within the first few nanometers from the metal surface. This reduces the overlap leading to a smaller MPG. The large discrepancies observed between cases (A) and (B) highlight the importance of accounting for the decay channels of the structure in the analysis of SPP amplification.

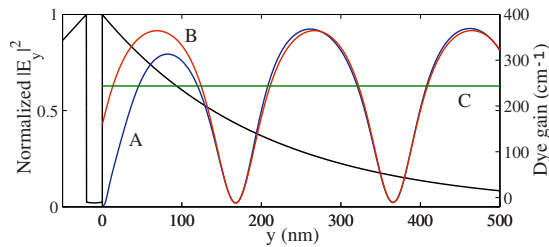


FIG. 4. (Color online) LRSPP mode and gain distributions for the cases under analysis.

Although small, the MPG for case (A) is still positive indicating net amplification. Moreover, larger MPG values seem to be practically attainable since we have assumed a modest R6G concentration and the assumed pump irradiance is well below the output of typical pulsed frequency-doubled Nd:YAG lasers. This suggests that lasing at visible wavelengths should be possible using the LRSPP mode of the proposed structure, provided that the cavity losses are not too high. In addition, the use of a finite width structure (i.e., a silver stripe)³¹ would relax the lasing requirements since the mode has a lower propagation loss and the field distribution overlaps better with the gain medium. On the other hand,

amplification of the SRSPP mode is quite challenging due to its large intrinsic propagation loss. For instance, considering case (A) one finds $\text{MPG} = -16438 \text{ cm}^{-1}$.

We note that our results are more optimistic than those reported by Winter *et al.*¹² The reason is because their model limits the gain available to the LRSPP to a fraction equal to the decay probability into this mode. Thus, following their approach, one realizes from Fig. 2(b) that the small decay probability into the LRSPP leads to a small amplification.

In summary, we proposed a theoretical model to describe the amplification of SPP modes in planar structures using optically pumped dipolar gain media. It accounts for the non-uniform gain distribution in close proximity to the metal and its overlap with the SPP mode. We apply the model to study the amplification of the LRSPP mode in a physically realizable structure using R6G molecules in solution as the gain medium. The results suggest that LRSPP net amplification in the visible is feasible using reasonable pump power and molecular concentration. The analysis shows that the gain non-uniformity close to the metal surface resulting from the position-dependent dipole lifetime and pump mechanism must be considered to describe adequately the SPP amplification phenomenon.

*ideleon@site.uottawa.ca

†berini@site.uottawa.ca

¹H. Raether, *Surface Plasmons on Smooth and Rough Surfaces and on Gratings* (Springer, Berlin, 1988).

²W. L. Barnes, A. Dereux, and T. W. Ebbesen, *Nature* (London) **424**, 824 (2003).

³G. A. Plotz, H. J. Simon, and J. M. Tucciarone, *J. Opt. Soc. Am.* **69**, 419 (1979).

⁴A. N. Sudarkin and P. A. Demkovich, *Sov. Phys. Tech. Phys.* **34**, 764 (1989).

⁵J. Seidel, S. Grafstrom, and L. Eng, *Phys. Rev. Lett.* **94**, 177401 (2005).

⁶M. A. Noginov, V. A. Podolskiy, G. Zhu, M. Mayy, M. Bahoura, J. A. Adegok, B. A. Ritzo, and K. Reynolds, *Opt. Express* **16**, 1385 (2008).

⁷I. Avrutsky, *Phys. Rev. B* **70**, 155416 (2004).

⁸S. A. Maier, *Opt. Commun.* **258**, 295 (2006).

⁹M. P. Nezhad, K. Tetz, and Y. Fainman, *Opt. Express* **12**, 4072 (2004).

¹⁰M. Z. Alam, J. Meier, J. S. Aitchison, and M. Mojahedi, *Opt. Express* **15**, 176 (2007).

¹¹T. Okamoto, F. H'Dhili, and S. Kawata, *Appl. Phys. Lett.* **85**, 3968 (2004).

¹²G. Winter, S. Wedge, and W. L. Barnes, *New J. Phys.* **8**, 125 (2006).

¹³A. Tredicucci, C. Gmachl, F. Capasso, J. E. Hutchison, D. L. Sivco, and A. Y. Cho, *Appl. Phys. Lett.* **76**, 2164 (2000).

¹⁴S. Anantha Ramakrishna and J. B. Pendry, *Phys. Rev. B* **67**, 201101(R) (2003).

¹⁵D. J. Bergman and M. I. Stockman, *Phys. Rev. Lett.* **90**, 027402

(2003).

¹⁶M. A. Noginov, G. Zhu, M. Bahoura, J. Adegok, C. E. Small, B. A. Ritzo, V. P. Drachev, and V. M. Shalaev, *Opt. Lett.* **31**, 3022 (2006).

¹⁷G. W. Ford and W. H. Weber, *Phys. Rep.* **113**, 195 (1984).

¹⁸A. Neogi, C. W. Lee, H. O. Everitt, T. Kuroda, A. Tackeuchi, and E. Yablonovitch, *Phys. Rev. B* **66**, 153305 (2002).

¹⁹K. T. Shimizu, W. K. Woo, B. R. Fisher, H. J. Eisler, and M. G. Bawendi, *Phys. Rev. Lett.* **89**, 117401 (2002).

²⁰Throughout the text we use the term irradiance to denote both the energy density flux of a standing wave and that of a running wave.

²¹A. Penzkofer and W. Leupacher, *J. Lumin.* **37**, 61 (1987).

²²M. Fischer and J. Georges, *Chem. Phys. Lett.* **260**, 115 (1996).

²³I. Z. Kozma, P. Krok, and E. Riedle, *J. Opt. Soc. Am. B* **22**, 1479 (2005).

²⁴J. J. Burke, G. I. Stegeman, and T. Tamir, *Phys. Rev. B* **33**, 5186 (1986).

²⁵E. D. Palik, *Handbook of Optical Constants of Solids* (Academic, New York, 1985).

²⁶F. Mikes, Y. Yang, I. Teraoka, T. Ishigure, Y. Koike, and Y. Okamoto, *Macromolecules* **38**, 4237 (2005).

²⁷L. G. Nair, *Prog. Quantum Electron.* **7**, 153 (1982).

²⁸P. Yeh, *Optical Waves in Layered Media* (Wiley, New York, 1988).

²⁹E. Hecht, *Optics*, 4th ed. (Addison-Wesley, Reading, MA, 2002).

³⁰C. Chen, P. Berini, D. Feng, S. Tanev, and V. Tzolov, *Opt. Express* **7**, 260 (2000).

³¹P. Berini, *Phys. Rev. B* **61**, 10484 (2000).